The Astrophysical Journal, 724:791–798, 2010 November 20 doi:10.1088/0004-637X/724/1/791

ON THE O/H, Mg/H, Si/H, AND Fe/H GAS AND DUST ABUNDANCE RATIOS IN GALACTIC AND EXTRAGALACTIC H II REGIONS*

Antonio Peimbert and Manuel Peimbert
Instituto de Astronomía, Universidad Nacional Autónoma de México, Apartado Postal 70-264, México 04510 D.F., Mexico; antonio@astroscu.unam.mx, peimbert@astroscu.unam.mx
Received 2010 June 2; accepted 2010 September 14; published 2010 November 4

ABSTRACT

We derive the Mg/H ratio in the Orion nebula and in 30 Doradus. We also derive the O/H and the Fe/O ratios in the extremely metal-poor galaxy SBS 0335−052 E. We estimate the dust depletions of Mg, Si, and Fe in Galactic and extragalactic H II regions. From these depletions we estimate the fraction of O atoms embedded in dust as a function of the O/H ratio. We find an increasing depletion of O with increasing O/H. The O depletion increases from about 0.08 dex, for the metal poorest H II regions known, to about 0.12 dex, for metal-rich H II regions. This depletion has to be considered to compare nebular with stellar abundances.

Key words: galaxies: abundances – galaxies: individual (SBS 0335–052) – galaxies: ISM – H II regions – ISM: abundances

1. INTRODUCTION

To determine the primordial helium abundance and to study the chemical evolution of galaxies it is necessary to derive the total $N(O)/N(H)$ ratio in H II regions; in this paper, the abundances are given by number following the usual definitions $X/H = 12 + \log N(X)/N(H)$, $X/O = \log N(X)/N(O) = X/H - O/H$, and $X^{+i}/H^{+} = 12 + \log N(X^{+i})/N(H^{+})$. To obtain the total O/H ratio in H II regions it is necessary to add the dust-phase to the gas-phase component of the O/H value. We presented elsewhere a preliminary discussion on the fraction of O trapped in dust grains (Peimbert & Peimbert 2010a). To find the fraction of O atoms embedded in dust grains we will estimate the depletions of Mg, Si, and Fe, and we will assume that the O atoms trapped in dust belong to molecules that include Mg, Si, and Fe atoms.

There are three results in favor of dust presence in low metallicity H II regions. (1) Cannon et al. (2002) found significant enhancements of the $I(H\alpha)/I(H\beta)$ value in some areas of I Zw 18 (one of the most metal-poor galaxies known) that are not due to underlying stellar absorption nor to the effect of collisional excitation of the Balmer lines; they conclude that the enhancements are more likely due to the presence of dust. (2) Thuan et al. (1997) find that dust is clearly present in the extremely metal-poor galaxy SBS 0335−052 E. (3) The Si/O versus O/H diagram of H II regions, where the Si/O ratio is almost independent of the O/H ratio and considerably smaller than the solar ratio implying that a substantial fraction of Si is embedded in dust grains (Garnett et al. 1995).

There are two arguments in favor of significantly lower depletion fractions of heavy elements into dust in metal-poor H II regions. (1) Izotov et al. (2006) find a slight increase of Ne/O with increasing metallicity, which they interpret as due to a moderate depletion of O onto grains in the most metal-rich galaxies; they conclude that this depletion corresponds to ∼20% of oxygen locked in the dust grains in the highest-metallicity H II regions of their sample, while no significant depletion would be present in the H II regions with lower metallicity. (2) Rodríguez & Rubin (2005) have estimated the fraction of Fe atoms in Galactic and extragalactic H II regions in the gaseous phase, and find that this fraction decreases with metallicity. The Fe depletions derived for the different objects define a trend of higher depletion at higher metallicities; while the Galactic H II regions show less than 5% of their Fe atoms in the gas phase, the low metallicity extragalactic regions (LMC 30 Doradus, SMC N88A, and SBS 0335−052 E) have somewhat lower fractions of Fe embedded in dust grains. Izotov et al. (2006) have produced an Fe/O versus O/H diagram that confirms the results by Rodríguez & Rubin.

To estimate the dust fraction as a function of O/H we need to have good gaseous abundance determinations for a relatively O-rich H II region; for this purpose, we will use the Orion nebula, its gaseous abundances derived by Esteban et al. (2004), and the result by Mesa-Delgado et al. (2009) that from three different methods have estimated that the fraction of O atoms trapped in dust in the Orion nebula amounts to 0.12 ± 0.03 dex. We will compare the Orion nebula abundances with the protosolar abundances by Asplund et al. (2009), and the solar vicinity B stars abundances by Przybilla et al. (2008).

Very O poor H II regions are also needed to find the fraction of O embedded in dust. Therefore, we decided to compute the O/H and Fe/H abundances of SBS 0335−052 E, and to consider results for other H II regions available in the literature.

In Sections 2 and 3, we determine the Mg/H value, adopt a set of O/H, Si/H, and Fe/H gaseous values, and estimate the fractions of O, Mg, Si, and Fe embedded in dust grains for the Orion nebula and for 30 Doradus, respectively. In Section 4, we compute the O/H and Fe/H abundances for SBS 0335−052 E based on the O/H abundances derived from recombination lines, considering the density dependence of the O II recombination lines, and the density dependence of the [Fe III] lines computed by Keenan et al. (2001). In Section 5, we make use of the Si/O ratios for five extragalactic H II regions obtained by Garnett et al. (1995). In Section 6, we compile Fe/O ratios from the literature for Galactic and extragalactic H II regions and estimate the Fe dust fraction as a function of O/H. In Section 7, we discuss the observational results and estimate the fraction of O atoms trapped in dust grains as a function of O/H, and the conclusions are presented in Section 8.

* Based on observations collected at the European Southern Observatory, Chile, proposal numbers ESO 68.C-0149(A) and ESO 69.C-0203(A).

Table 1
Gas and Dust Abundances[a] for the Solar Vicinity and the Orion Nebula

Element	Protosolar[b]	Protosolar + GCE[b,c]	B Stars Solar Vicinity[d]	ISM Solar Vicinity[e]	Orion g + d[f]	Orion Gas[g]	Orion Gas Fraction (%)	Orion Dust Fraction (%)
O	8.73 ± 0.05	8.82 ± 0.06	8.76 ± 0.03	8.79 ± 0.03	8.77 ± 0.03	8.65 ± 0.03	(76 ± 5)	(24 ± 5)
Mg	7.64 ± 0.04	7.73 ± 0.07	7.56 ± 0.05	7.64 ± 0.08	(7.62 ± 0.05)	6.56 ± 0.16	(9 ± 3)	(91 ± 3)
Si	7.55 ± 0.04	7.68 ± 0.09	7.50 ± 0.02	7.59 ± 0.09	(7.56 ± 0.04)	6.94 ± 0.12	(24 ± 7)	(76 ± 7)
Fe	7.54 ± 0.04	7.74 ± 0.14	7.44 ± 0.04	7.59 ± 0.15	(7.55 ± 0.04)	6.07 ± 0.20	(3^{+2}_{-1})	(97^{+1}_{-2})

Notes.
[a] Abundances in units of 12 + log $N(X)/N(H)$.
[b] Protosolar values from Asplund et al. (2009).
[c] Galactic chemical evolution correction from Carigi (1996), Chiappini et al. (2003), and Carigi & Peimbert (2008, 2010), see the text.
[d] Solar vicinity B stars from Przybilla et al. (2008).
[e] Adopted solar vicinity ISM abundances, average from B stars and protosolar values corrected for Galactic chemical evolution.
[f] O from Esteban et al. (2004) including the dust correction from Mesa-Delgado et al. (2009); values in parentheses come from the ISM solar vicinity values presented in the fifth column and a small correction due to the larger galactocentric distance of Orion relative to the Sun predicted by the Galactic chemical evolution models mentioned above.
[g] O from Esteban et al. (2004), Fe from Esteban et al. (1998), and Mg and Si from this paper.

2. THE ORION NEBULA

In Table 1, we present the solar neighborhood and Orion Nebula abundances that will be used as reference values to estimate the fraction of a given element in the dust phase. In Column 2, we present the protosolar abundances (Asplund et al. 2009). In Column 3, we present the solar neighborhood abundances by correcting the protosolar abundances due to the chemical evolution of the Galaxy since the Sun was formed; based on the Galactic chemical evolution models of Carigi (1996), Chiappini et al. (2003), and Carigi & Peimbert (2008, 2010) we added 0.09, 0.09, 0.13, and 0.20 dex to the protosolar values of O, Mg, Si, and Fe, respectively. In Column 4, we present the chemical abundances derived by Przybilla et al. (2008) from six B stars of the solar vicinity; Simón-Díaz (2010) has recently derived the O and Si abundances for 13 B stars from the Orion region, his results are in very good agreement with those by Przybilla et al.; note that B star abundances do not need correction for Galactic chemical evolution since these stars are only a few million years old. In Column 5, we present our adopted abundances for the interstellar medium (ISM) of the solar vicinity; we obtained these values from a simple average of Columns 3 and 4. In Column 6, we present the expected total abundances for the Orion Nebula; we obtained these values by considering the different galactocentric distances of the solar vicinity and the Orion Nebula and subtracting to the O, Mg, Si, and Fe solar neighborhood abundances 0.02, 0.02, 0.03, and 0.04 dex, respectively, to account for the presence of Galactic abundance gradients; the Galactic gradients are obtained from the Galactic chemical evolution models by Carigi, Chiappini, and their collaborators; it is worth mentioning that the expected total, gas plus dust, O/H value for the Orion nebula is equal to the total derived O/H value from observations by Mesa-Delgado et al. (2009) (see below). In Column 7, we present the gaseous abundances of the Orion nebula; the O/H abundance comes from Esteban et al. (2004), the Fe/H abundance from Esteban et al. (1998), and the Mg/H and Si/H abundances from this paper (see below).

Baldwin et al. (1991) estimated an upper limit to the gaseous Mg/H value of 6.58 dex from an upper limit to the Mg II λ2800/Hβ line intensity ratio obtained by Perinotto & Patriarchi (1980). From the same raw data of the observations for Orion by Esteban et al. (2004), we have estimated the gaseous Mg abundance in this region. From these data, we have measured the following line ratios: $I(4481.22, \text{Mg II})/I(\text{H}\beta) = (3.6 \pm 1.6) \times 10^{-5}$ and $I(4482.17, \text{Fe I}])/I(\text{H}\beta) = (8.6 \pm 2.5) \times 10^{-5}$. As we can see in Figure 1, high-resolution spectra are needed to separate the Mg II line from the 4482.2 line, that is probably due to the Fe I] (a^5–z^7F^0). Under the assumption that the Mg II 3*d*–4*f* λ4481 line has an effective recombination coefficient equal to that of the C II 3*d*–4*f* λ4267 line (Liu et al. 2004), from the Mg II/Hβ intensity ratio and the C II line effective recombination coefficient we derive a gaseous Mg^{++}/H^+ value of 6.54 ± 0.16 dex. By adding 0.02 dex due to the presence of Mg^+ (Baldwin et al. 1991), we obtain a total Mg/H gaseous component of 6.56 ± 0.16 dex. Our Mg/H ratio is in agreement with the upper limit obtained by Baldwin et al., this ratio together with the reference stellar value of Table 1, implies that (9 ± 3)% of the Mg atoms are in gaseous form and (91 ± 3)% are embedded in dust.

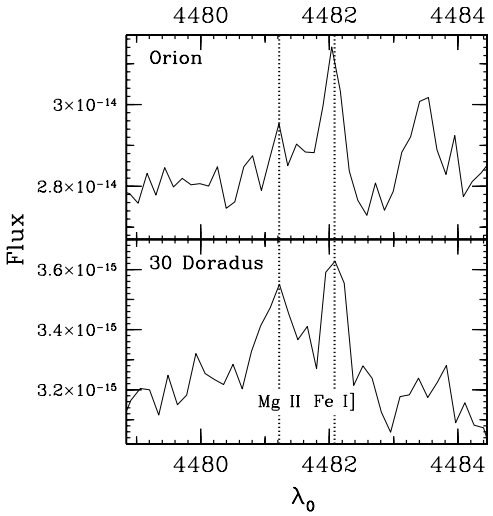

Figure 1. Spectra of the Orion nebula and the 30 Doradus nebula that show the λλ4481.22, Mg II and 4482.17, Fe I] emission lines, the rest wavelength is given in Angstroms and the flux in erg cm^{-2} s^{-1} A^{-1}.

Garnett et al. (1995) obtained UV observations of the Orion nebula with the *Hubble Space Telescope* and found that Si/C = −1.46 ± 0.10 dex. From the C/O value of −0.25 dex

derived by Esteban et al. (2004) and the previous result we find that the gaseous Si/O value amounts to −1.71 dex. By considering that 0.12 dex of O is tied up in dust grains it follows that the gaseous Si to the total (gas + dust) O abundance is equal to −1.83 dex, and consequently that Si/H = 6.94 ± 0.12 dex. This number together with the reference Si/H value implies that the fraction of Si atoms tied up in dust grains amounts to 76% in the Orion nebula (see Table 1). Similarly Esteban et al. (1998) obtained that the gaseous Fe/H = 6.07 ± 0.20 dex, this result together with the Fe/H reference value implies that about 97% of the Fe atoms are tied up in dust grains.

The total O value for the Orion nebula presented in Table 1, O/H = 8.77 dex, was obtained from two different methods: (1) by adding to the gaseous value derived by Esteban et al. (2004) for $t^2 = 0.022$ the dust correction of 0.12 dex estimated by Mesa-Delgado et al. (2009), where t^2 is the mean square temperature variation (Peimbert 1967), and (2) by using the same procedure for O as the one used for the other elements of Table 1.

The use of the t^2 formalism presented by Peimbert (1967) and Peimbert & Costero (1969) will be used throughout this paper. As mentioned before the use of $t^2 = 0.022$ gives O/H = 8.65, a reasonable value for the estimated oxygen depletion. On the other hand, under the simpler assumption that H II regions have uniform temperature ($t^2 = 0.000$), Deharveng et al. (2000), Pilyugin et al. (2003), and Esteban et al. (2004) obtain for the Orion nebula O/H values of 8.51, 8.49, and 8.51 dex, respectively, a difference of 0.27 dex with respect to the total oxygen value presented in Table 1, a difference too large to be explained by the depletion of oxygen into dust grains. It should be noted that of the well-observed H II regions the Orion nebula presents one of the lowest t^2 values (e.g., Esteban et al. 2002, 2005, 2009; Peimbert 2003; Peimbert et al. 2007; García-Rojas et al. 2007), therefore in general we expect larger abundance differences than in Orion between the $T(4363/5007)$ method and the method with t^2 values different from zero.

We will assume that the fraction of O atoms tied up in dust grains of H II regions is proportional to the fraction of atoms of Mg, Si, and Fe tied up in dust grains of each nebula and that the constant of proportionality will be given by the Orion nebula results. This assumption is a first approximation to this problem and is based on the following ideas: (1) as far as molecules—that survive as part of dust grains in an H II region—go, the elements that most frequently bind with O atoms are Mg, Si, and Fe; (2) Na, Al, Ca, Cr, Mn, and Ni are less abundant than the previous three elements, and most of them have similar behaviors to those of either Mg, Si, or Fe; (3) the O atoms tied up by Mg, Si, and Fe are present in molecules like [(Mg,Fe)$_2$SiO$_4$] and [(Mg,Fe)SiO$_3$] (Ossenkopf et al. 1992); Fe$_2$O$_3$ and Fe$_3$O$_4$ (Nuth & Hecht 1990); and MgO (Fadeyev 1988); and (d) in these molecules about one O atom is attached to an Mg, Si, or Fe atom.

For the Orion Nebula we know that $N(\mathrm{O_{dust}})/N(\mathrm{O_{total}}) = 0.241 \pm 0.060$. From this result, the previous assumption, and the values of Table 1 we obtain that

$$\frac{N(\mathrm{O})_{\mathrm{dust}}}{N(\mathrm{O})_{\mathrm{total}}} = (0.241 \pm 0.060)\frac{\left[\frac{N(\mathrm{Mg})_{\mathrm{dust}}}{N(\mathrm{Mg})_{\mathrm{total}}} + \frac{N(\mathrm{Si})_{\mathrm{dust}}}{N(\mathrm{Si})_{\mathrm{total}}} + \frac{N(\mathrm{Fe})_{\mathrm{dust}}}{N(\mathrm{Fe})_{\mathrm{total}}}\right]}{2.64}. \quad (1)$$

The error bars from Equation (1) correspond to a systematic uncertainty that depends on the exact O depletion of the Orion Nebula; we will ignore this systematic error for most of the paper and will look into it at the end of Section 7.

We will estimate the $\mathrm{O_{total}}$ for other H II regions from Equation (1) and the next equation:

$$\left[\frac{N(\mathrm{O})}{N(\mathrm{H})}\right]_{\mathrm{total}} = \frac{1}{1-0.2739}\left(\left[\frac{N(\mathrm{O})}{N(\mathrm{H})}\right]_{\mathrm{gas}} - 0.0913\left\{\frac{\left[\frac{N(\mathrm{Mg})}{N(\mathrm{H})}\right]_{\mathrm{gas}}}{\left[\frac{N(\mathrm{Mg})}{N(\mathrm{O})}\right]_{\mathrm{ref}}} + \frac{\left[\frac{N(\mathrm{Si})}{N(\mathrm{H})}\right]_{\mathrm{gas}}}{\left[\frac{N(\mathrm{Si})}{N(\mathrm{O})}\right]_{\mathrm{ref}}} + \frac{\left[\frac{N(\mathrm{Fe})}{N(\mathrm{H})}\right]_{\mathrm{gas}}}{\left[\frac{N(\mathrm{Fe})}{N(\mathrm{O})}\right]_{\mathrm{ref}}}\right\}\right). \quad (2)$$

Jenkins (2009) finds for some lines of sight of the ISM, that include mainly neutral material, that the O depletion reaches values in the 0.2–0.3 dex range. He concludes that O molecules that include Mg, Si, and Fe are not enough to account for these depletions and suggests that ices might also be present. Equations (1) and (2) were calibrated with the Orion nebula, where according to Mesa-Delgado et al. (2009) the O depletion derived from the assumption that O is trapped by molecules, that include only Mg, Si, and Fe, agrees with (1) the O depletion estimated from the comparison of the stellar abundances of the Orion region with the nebular abundances, and (2) with the O pre-shock nebular abundances and post-shock O abundances associated with the H–H object 202, in this object after the shockwave passes dust grains are destroyed and most of the Fe trapped in grains is returned to the gaseous phase, they assume also that most of the O is returned to the ISM. Since the Orion nebula is one of the H II regions with the highest Fe depletion we consider it unlikely that the O depletions of H II regions with lower Fe depletions are higher than in the Orion nebula, therefore, we conclude that ices and O_2 molecules are practically absent in H II regions.

3. THE 30 DORADUS NEBULA

To obtain the fraction of O, Mg, Si, and Fe in the dust phase of 30 Doradus we will follow the same procedure as for the Orion nebula.

Based on the raw data presented by Peimbert (2003) we derived these two line ratios: $I(4481.22,\ \mathrm{Mg\,II})/I(\mathrm{H}\beta) = (1.11 \pm 0.28) \times 10^{-4}$ and $I(4482.17,\ \mathrm{Fe\,I])}/I(\mathrm{H}\beta) = (1.06 \pm 0.27) \times 10^{-4}$, the observed Mg II and Fe I] lines are presented in Figure 1. From the 4481 Mg II line intensity we obtained that $\mathrm{Mg^{++}/H^{+}} = 7.06 \pm 0.12$ dex. The Mg/H total gaseous value is presented in Table 2, due to the considerably higher degree of ionization of 30 Doradus relative to the Orion nebula we neglected the contribution to this value due to $\mathrm{Mg^{+}}$.

Tsamis & Péquignot (2005), from the observations of λλ4561 and 4571 of Mg I] by Peimbert (2003), also derived the Mg/H value for 30 Doradus and it is presented in Table 2. To obtain a representative average of the two sets of values, we normalized them by matching the two O/H values and consequently we added 0.05 dex to the O/H, Mg/H, Si/H, and Fe/H gaseous determinations by Tsamis and Péquignot and averaged them with the O and Fe determinations by Peimbert (2003), the Si determination by Garnett et al. (1995), and the Mg determination presented in this paper (see Table 2).

We adopted for 30 Doradus the Mg/O, Si/O, and Fe/O reference values of the Orion nebula. From these values, the observed gas phase Mg/H, Si/H, and Fe/H abundances, and Equation (2), we derived the O/H total value. By comparing the total gaseous abundances with the reference values presented in Table 2 we derived the fractions of the Mg, Si, and Fe atoms in the gas phase and the dust phase. The 30 Doradus Mg and Fe fractions are slightly lower than those of Orion, while Si

Table 2
Gas and Dust Abundances[a] for 30 Doradus

Element	Gas[b]	Gas[c]	Gas[d]	g + d[e]	Gas Fraction (%)	Dust Fraction (%)
O	8.50 ± 0.05	8.45 ± 0.05	8.50 ± 0.05	8.61 ± 0.03	(78 ± 5)	(22 ± 5)
Mg	7.06 ± 0.10	6.69 ± 0.16	6.90 ± 0.13	(7.46 ± 0.05)	(28 ± 9)	(72 ± 9)
Si	6.80 ± 0.27	6.50 ± 0.27	6.68 ± 0.27	(7.40 ± 0.04)	(19^{+16}_{-9})	(81^{+16}_{-9})
Fe	6.39 ± 0.20	6.12 ± 0.20	6.28 ± 0.20	(7.39 ± 0.04)	(8^{+4}_{-3})	(92^{+4}_{-3})

Notes.
[a] Abundances in units of $12 + \log N(\mathrm{X})/N(\mathrm{H})$.
[b] Gaseous abundances for $t^2 = 0.033$. O and Fe from Peimbert (2003). Si from Garnett et al. (1995). Mg from this paper.
[c] Gaseous abundances for the inhomogeneous model by Tsamis & Péquignot (2005).
[d] Adopted gaseous abundances from the average of the previous two columns, where all the values of the previous column were increased by 0.05 dex (see the text).
[e] Reference gas plus dust abundances, given in parentheses, come from the X/O values of Table 1. The total O abundance was derived from Equation (2).

is nearly constant; this result gives us an initial hint that the fraction of heavy elements trapped in dust diminishes at lower metallicities.

4. THE FE/H AND O/H RATIOS IN SBS 0335−052 E

It is important to obtain the Fe/O and the O/H ratio of the metal poorest H II regions to try to find out if a substantial fraction of Fe is tied up in dust grains and consequently also a non-negligible amount of O atoms. To reach this objective we will compute the abundances for SBS 0335−052 E.

4.1. The Fe/H ratio

Recently Izotov et al. (2009) derived the Fe/H value for SBS 0335−052 E from observations obtained with UVES and FORS. On the one hand, their results based on the λ4987 [Fe III] line need to be corrected because with the FORS resolution the line is a blend of λλ4986+4987, and the contribution of λ4986 has to be taken into account due to the large intensity of this line at low densities. We have obtained a density value of 108 ± 12 cm^{-3} for SBS 0335−052E from Figure 2—where we present the $I(4986)/I(4658)$ and $I(4987)/I(4658)$ ratios as a function of density—and the [Fe III] line intensities of this object measured by Izotov et al. (2009). On the other hand, the Fe values derived from 4658 are almost density independent. From the $I(4658)$ observations in SBS 0335−052 E Izotov et al. (2009) obtain an Fe/O = −1.36 ± 0.03 dex in the gas phase.

To calculate the total fraction of Fe in dust grains, we first need to obtain the $\mathrm{Fe_{gas}/O_{total}}$ value and then compare it to the reference value. To correct for the fraction of O in dust grains we will use Equation (2) and the reference values derived for the Orion nebula. The gaseous Si/O ratio comes from Garnett et al. (1995) who obtain Si/O = −1.72 ± 0.20 dex. We will assume that the value of the Mg term of Equation (2) lies between the values of the Si and Fe terms, we will discuss this point further in Section 7. From the previous considerations we derive a correction of 0.08 ± 0.01 dex for the O abundance. Therefore, we obtain an $\mathrm{Fe_{gas}/O_{total}}$ of −1.44±0.03 dex. Taking as reference value the solar vicinity ISM abundances, the Fe/O ratio amounts to −1.20 ± 0.15 dex, and we obtain that the fraction of Fe in gaseous form amounts to (58 ± 20)% and that the rest is trapped in dust grains.

4.2. The O/H ratio

Due to the presence of temperature inhomogeneities the abundances derived from $T(4363/5007)$ and the [O III] lines

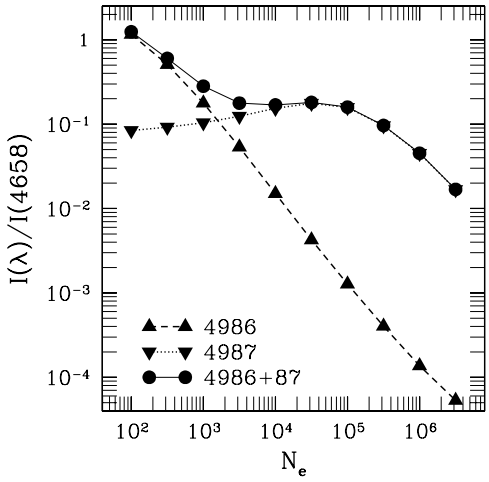

Figure 2. [Fe III] line intensity ratios. $I(\lambda)/I(4658)$ vs. N_e for $T_e = 15{,}000$ K from the computations by Keenan et al. (2001).

are only lower limits to the O/H value. Therefore, it is very important to obtain the O abundances from recombination lines that are independent of the temperature structure. Moreover, the combination of the forbidden and permitted lines of O allows us to estimate the value of t^2.

To derive an accurate O/H value it is also necessary to consider the density dependence of the O II lines. The sum of the intensities of all the lines of the O II multiplet 1, I(total), has a temperature and density dependence that is proportional to $T^{-0.9}N^2$, similar to the temperature and density dependence of the H I lines. However, the fraction of the intensity due to each one of the lines of the O II multiplet 1 varies when $N_e < 10{,}000$ cm^{-3}. In Figure 3, we present the density dependence of the eight O II lines of multiplet 1 that were obtained empirically from observations of planetary nebulae and H II regions (Ruiz et al. 2003; Peimbert & Peimbert 2005; Peimbert et al. 2005). Bastin & Storey (2006) from atomic physics computations obtain a similar behavior for the $I(4649)/I$(total) versus density relation to that derived empirically from observations.

To obtain abundances from the O recombination lines it is necessary to take into account the possible blend of the O II lines when the resolution is not high enough. From the equations by Ruiz et al. (2003), Peimbert & Peimbert (2005), and Peimbert et al. (2005), for those cases where the resolution is of the order

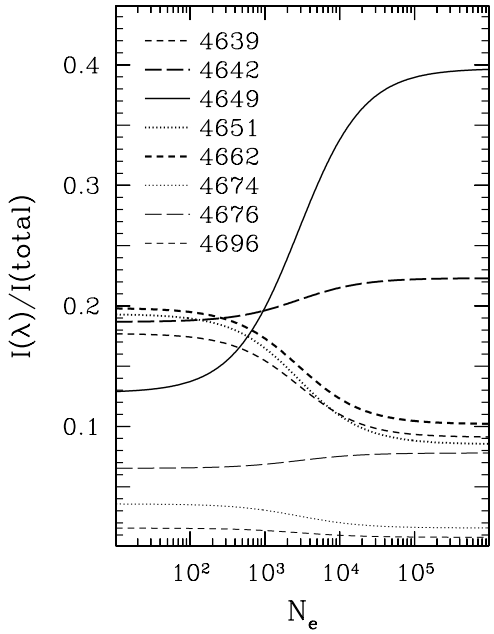

Figure 3. $I(\lambda)/I(\mathrm{total})$ vs. N_e for the O II line intensities, based on the equations derived from observations by Ruiz et al. (2003), Peimbert & Peimbert (2005), and Peimbert et al. (2005).

of 2–3 Å, we recommend the following equations:

$$\left[\frac{I(4639+42)}{I(\mathrm{total})}\right]_{\mathrm{obs}} = 0.315 + \frac{0.051 \pm 0.008}{[1 + N_e(\mathrm{FL})/1325]}, \quad (3)$$

$$\left[\frac{I(4649+51)}{I(\mathrm{total})}\right]_{\mathrm{obs}} = 0.482 - \frac{0.170 \pm 0.011}{[1 + N_e(\mathrm{FL})/1325]}, \quad (4)$$

and

$$\left[\frac{I(4674+76)}{I(\mathrm{total})}\right]_{\mathrm{obs}} = 0.093 + \frac{0.007 \pm 0.003}{[1 + N_e(\mathrm{FL})/1325]}. \quad (5)$$

In Figure 4, we present what fraction of the total intensity is present in each of these blends as a function of density.

Due to the importance and the faintness of the O II recombination lines we decided to reduce the FORS raw data for SBS 0335−052 E present in the VLT archive; an independent reduction of these data was made by Izotov et al. (2009). We obtain that $I(4649+51)/I(\mathrm{H}\beta)$ amounts to 0.0132 ± 0.0074, in addition we obtain that $I(4639+42)/I(\mathrm{H}\beta)$ amounts to 0.0085 ± 0.0074. From our two measurements we find that $I(4639 + 4641 + 4649 + 51)/I(\mathrm{H}\beta) = 0.0217 \pm 0.0104$. We have subtracted to $I(\mathrm{H}\beta)$ the contribution due to collisional excitation, that according to Peimbert et al. (2007) amounts to 6.6%, and obtain that $I(4639+4641+4649+51)/I(\mathrm{H}\beta)_{\mathrm{rec}} = 0.0231 \pm 0.0111$. Based on the $I(4639+42)/I(4649+51)$ line ratio and the very low N/O ratio in this object we consider that the feature at λλ4639+4642 is due to the O II lines and not to the 4642 N III line, contrary to the suggestion by Izotov et al. (2009).

From our measurements, Equations (3) and (4), the recombination coefficients of O II by Storey (1994), and the H I recombination coefficients by Storey & Hummer (1995) we obtain an abundance of $\mathrm{O}^{++}/\mathrm{H}^{+} = 7.36^{+0.17}_{-0.28}$ dex. The total O/H value amounts to $7.41^{+0.17}_{-0.28}$ dex and includes the O^{+} contribution that amounts to 0.05 dex (Luridiana et al. 2003; Izotov et al. 2009). Our O/H value can be compared with the values for $t^2 = 0.00$ derived by Peimbert et al. (2007) and Izotov et al. (2009) that amount to 7.31 ± 0.04 dex and 7.23 ± 0.01 dex, respectively, and also with the value derived by Peimbert et al. for $t^2 = 0.04$ that amounts to 7.47 ± 0.04 dex. In Table 3, we present the value for $t^2 = 0.00$ by Peimbert et al. (2007), we also present the O/H value derived by Peimbert et al. for $t^2 = 0.04$.

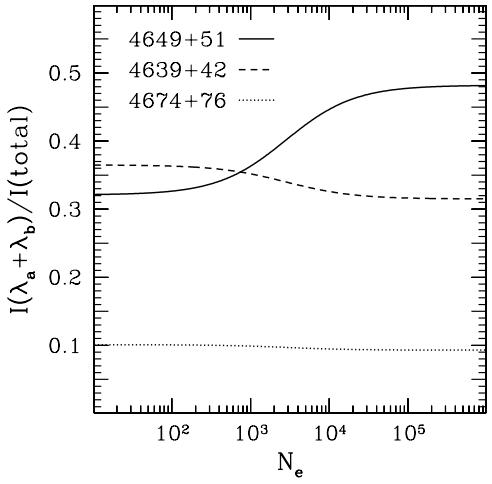

Figure 4. $I(\lambda_a + \lambda_b)/I(\mathrm{total})$ vs. N_e, based on Equations (3)–(5).

From the FORS raw data for SBS 0335 −052 E Izotov et al. (2009) obtain that $I(4649+51)/I(\mathrm{H}\beta) = 0.02 \pm 0.01$. From this line intensity ratio they obtain that $\mathrm{O}^{++}/\mathrm{H}^{+} = 7.18^{+0.17}_{-0.30}$ dex, and by adding the O^{+} contribution a total $\mathrm{O/H} = 7.23^{+0.17}_{-0.30}$ dex. From their published line intensity, the recombination coefficients by Storey (1994), and Storey & Hummer (1995), and Equation (4) we derive an $\mathrm{O}^{++}/\mathrm{H}^{+}$ abundance of 7.62 dex and by adding the O^{+} contribution a total O/H = 7.67 dex. The lower O/H value derived by Izotov et al. (2009) is not correct, their result probably has been affected by at least one of the following causes: (1) that they did not consider the density dependence of the O II lines and (2) that they did not use the proper branching ratio for the O II lines.

5. THE Si/O RATIO IN H II REGIONS

Si and O are produced by core collapse supernovae and this production is expected to be independent of the O/H ratio. By comparing the Si/O ratio in H II regions with the Si/O ratio in B stars of the solar vicinity it is possible to estimate the fraction of Si in gas and dust phases in H II regions.

Garnett et al. (1995) derived the Si/O ratio for eight Galactic and extragalactic H II regions with gaseous O/H abundances in the 7.2–8.7 dex range and found that the Si/O ratio was almost constant for these objects. From the Orion and 30 Doradus data of Sections 2 and 3, and the data of the other six objects of Garnett et al. (see Table 3), we derived an average gaseous $\mathrm{Si_{gas}/O_{gas}} = -1.66 \pm 0.05$ dex. The $\mathrm{Si_{gas}/O_{total}}$ versus $\mathrm{O_{total}/H}$ for the eight H II regions discussed in this paper is presented in Figure 5.

The reference value for Si/O amounts to −1.20 dex and is obtained from the protosolar + GCE Si/O value (Asplund et al. 2009; Chiappini et al. 2003; Carigi & Peimbert 2008, 2010) and the Si/O B stars values (Przybilla et al. 2008) that amount to −1.14 dex and −1.26 dex, respectively.

Since the Orion nebula, the metal richest H II region of the sample, has an oxygen depletion of 0.12 dex, and SBS 0335 − 052 E, one of the two metal poorest H II regions of the sample,

Table 3
O/H Visual and Si/O UV Values

Value	SMC N88A	NGC 2363	C1543+091	T1214 − 277	SBS 0335− 052 E	I Zw 18
$O_{gas}/H; t^2 = 0.00$[a]	8.06 ± 0.04	7.92 ± 0.04	7.76 ± 0.10	7.59 ± 0.04	7.31 ± 0.04	7.18 ± 0.04
$O_{gas}/H; t^2 \neq 0.00$[a]	8.13 ± 0.10	8.00 ± 0.06	7.91 ± 0.10	7.74 ± 0.10	7.47 ± 0.04	7.29 ± 0.05
Si_{gas}/O_{gas}[b]	−1.74 ± 0.12	−1.59 ± 0.14	−1.74 ± 0.14	−1.46 ± 0.28	−1.72 ± 0.20	−1.52 ± 0.22
$O_{total}/H; t^2 \neq 0.00$[c]	8.23 ± 0.10	8.10 ± 0.07	8.01 ± 0.10	7.84 ± 0.10	7.51 ± 0.05	7.38 ± 0.05
Si_{gas}/O_{total}[c]	−1.84 ± 0.12	−1.69 ± 0.14	−1.84 ± 0.14	−1.56 ± 0.28	−1.80 ± 0.20	−1.61 ± 0.22
Si gas fraction[d]	(23 ± 6)%	(32 ± 10)%	(23 ± 7)%	(44^{+39}_{-20})%	(25^{+15}_{-9})%	(39^{+26}_{-16})%

Notes.
[a] Garnett et al. (1995), Peimbert et al. (2000, 2007) and this paper.
[b] Garnett et al. (1995).
[c] This paper, oxygen dust fraction from Sections 4 and 8.
[d] Under the assumption of a reference value of $Si_{total}/O_{total} = -1.20$ dex.

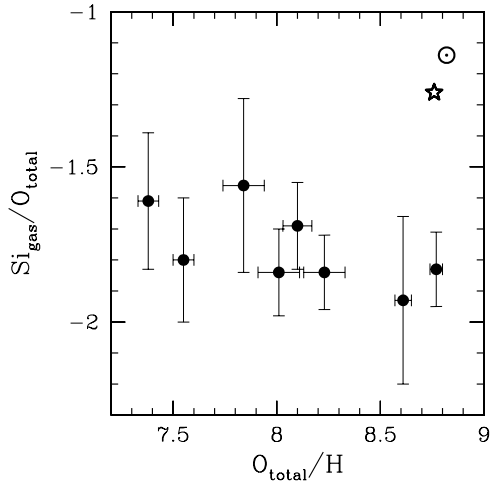

Figure 5. Si_{gas}/O_{total} vs. O_{total}/H. The star represents the B stars of the solar vicinity, the open circle with the central dot the protosolar + GCE value, and the filled circles the extragalactic H II regions (see Tables 1 and 3).

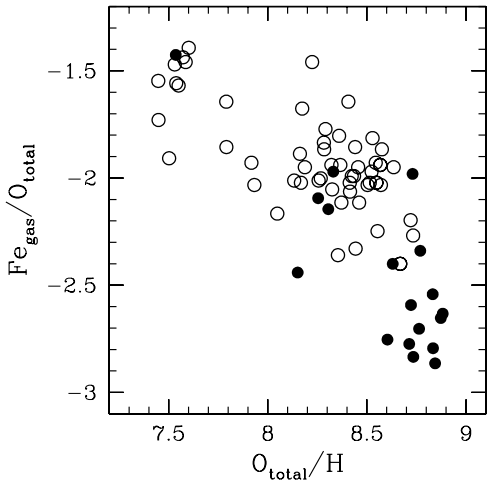

Figure 6. Fe_{gas}/O_{total} vs. O_{total}/H, where to derive the O_{total} from Equation (2) we have assumed that the fraction of Si in gas phase amounts to 28%, that the fraction of Mg in gas phase is intermediate between those of Si and Fe, and that the reference value for Fe_{total}/O_{total} is −1.20 dex. The open circles come from measurements by Izotov et al. (1997, 1999) and Izotov & Thuan (1998, 2004), where the O/H values have been corrected for the presence of temperature variations, see the text. The filled circles are from measurements by Esteban et al. (2002, 2004, 2009), García-Rojas et al. (2004, 2005, 2006, 2007), Peimbert et al. (2000), and this paper, where the O/H values come from recombination lines.

has an oxygen depletion of 0.08 dex, we can assume that most of the H II regions have an intermediate depletion value. As a first approximation we will adopt 0.10 dex for the fraction of O trapped in dust grains. In Section 7, this point will be discussed further and we will see that 0.10 dex is a good representative value for most H II regions.

From the previous considerations, we estimate that the average ratio of Si_{gas}/O_{total} amounts to −1.76 dex, from this estimate and the reference value of Si_{total}/O_{total} of −1.20 dex we obtain that in H II regions, about 28% of the Si is in the gas phase and 72% in the dust phase.

Note that the specific correction for oxygen in dust grains for the objects in Table 3 (except SBS 0335−052 E) follow the recipe derived in Section 8.

6. THE Fe/O RATIO IN H II REGIONS

In Figure 6, we present the Fe/O versus O/H ratio compiled from many sources in the literature. The data come from two different sets. In the first set, the O/H determination comes from recombination line ratios which are independent of the temperature structure. In the second one, the O/H ratios are derived in the traditional way, this depends on the ratio of collisionally exited to recombination lines which is strongly dependent on the temperature structure of the H II region (Peimbert 1967; Peimbert & Costero 1969; Peimbert & Peimbert 2010b).

To correct for the presence of temperature variations we have added 0.24 dex to the O/H ratio, this correction comes from the average value of 13 well-observed extragalactic H II regions (Esteban et al. 2002, 2009; López-Sánchez et al. 2007). Note that the Fe/O ratio is almost independent of the temperature structure since it is determined from a ratio of collisionally excited lines that show a similar temperature dependence.

Part of the scatter in Figure 6 could be due to errors in the determinations of the gas-phase Fe/O ratios and part to the different star formation histories of the different galaxies. The closer in time to a recent burst of star formation the lower the total Fe/O ratio in their ISM. In the solar vicinity at present all the O abundance is due to core collapse supernovae, while about 40% of the Fe is due to core collapse supernovae and the other 60% to Type Ia supernovae (e.g., Pagel & Tautvaisiene 1995; Pagel 2009). There is a time delay in the Fe formation relative to the O formation, and consequently the Fe/O ratio depends on the star formation rate, the initial stellar mass function, and the gas flows from and into the intergalactic medium. There are two well-established Fe/O ratios from observations: the one when the Sun was formed, called the protosolar ratio that amounts to

−1.19 dex (Asplund et al. 2009), and the present value in the solar vicinity based on observations of B stars that amounts to −1.32 dex (Przybilla et al. 2008); from the protosolar value plus the modification due to Galactic chemical evolution we find a value of Fe/O = −1.08 dex for the present ISM (see Table 1). From the average of the previous two values we obtain an Fe/O = −1.20 dex.

From Figure 6 and under the assumption that the total Fe/O ratio amounts to −1.20 dex, we obtain that for the Galactic and extragalactic H II regions with abundances in the 8.3 dex < O/H < 8.8 dex range the average fraction of Fe in the gaseous phase is about 10%, with some of them reaching 3%. For the extragalactic H II regions with abundances in the 7.8 dex < O/H < 8.3 dex range the fraction of Fe in the gaseous phase is about 25%. For the extragalactic H II regions in the 7.3 dex< O/H < 7.8 dex range the fraction of Fe in the gaseous phase is about 50%.

7. DISCUSSION

The Fe/O variation as a function of O/H implies that in the high metallicity high-density Galactic H II regions about 97% of the Fe atoms are embedded in dust grains. This fraction diminishes with diminishing O/H and in the metal poorest extragalactic H II regions, characterized by high electron temperature and low electron density, about 40% of the Fe atoms are embedded in dust grains. The Si/O ratio is approximately constant from the O richest to the O poorest H II regions, implying that for the whole O/H observed range the fraction of Si embedded in dust grains amounts to about 72% ± 10%. A possible explanation for these two results is that dust grains have a solid core with about 72% of the Si and about 40% of the Fe atoms present in the ISM, and that in addition they have a softer mantle with about 57% of the Fe present in the ISM. The softer mantle is destroyed at higher temperatures and lower densities, while the solid core remains intact in all the H II regions of the sample.

We have only the estimate of Mg_{gas}/H for the Orion nebula and for 30 Doradus. The 30 Doradus results imply that Mg_{gas}/H is similar to Si_{gas}/H and a lot larger than Fe_{gas}/H. For the Orion nebula the Mg_{gas}/H is intermediate between Si_{gas}/H and Fe_{gas}/H. Jenkins (2009) finds that in lines of sight dominated by neutral material the Mg and Si depletions are very similar and considerably smaller than those of Fe. From these results, we will explore two possibilities for the H II region set: (1) that Mg_{gas}/H is equal to Si_{gas}/H, and (2) that Mg_{gas}/H is intermediate between Si_{gas}/H and Fe_{gas}/H.

We found that in the range of metallicities studied here there is a small but measurable trend in the sense that the depletion of O in dust grains increases with metallicity. The limiting values for the O depletion are 0.08 dex for the O poorest objects, based on the observations of SBS 0335 − 052 E, one of the O poorest objects known; and 0.12 dex for the Orion nebula, one of the richest objects with a good determination. Note that the upper limit given by Equation (1) is 0.14 dex if no Mg, Si, or Fe atoms remain in the gas phase.

We decided to divide the sample into three O/H groups: (1) 7.3 < O/H < 7.8 dex, (2) 7.8 < O/H < 8.3 dex, and (3) 8.3 dex < O/H < 8.8 dex. We took the Fe_{gas}/O_{total} average of all the H II regions in each interval as representative of each group, and from Equation (1) we computed Table 4. In the first row of Table 4, we present the O depletions, under the assumption that the ISM reference values are given by Mg/O = −1.15 dex, Si/O = −1.20 dex, and Fe/O = −1.20 dex, and that Mg_{gas}/H is equal to Si_{gas}/H; in the second row of Table 4, we have assumed that Mg_{gas}/H is intermediate between to the Si_{gas}/H and Fe_{gas}/H. Finally, in the last row of Table 4 we present our adopted values.

Table 4
Depletion of O in Dust Grains (dex)

Mg_{gas}/H Assumption	Low O/H[a]	Intermediate O/H[b]	High O/H[c]
Si_{gas}/H behavior[d]	0.087 ± 0.004	0.100 ± 0.005	0.105 ± 0.006
Intermediate behavior[d,e]	0.084 ± 0.005	0.101 ± 0.006	0.108 ± 0.007
Adopted[f]	0.09 ± 0.01	0.10 ± 0.01	0.11 ± 0.01

Notes.
[a] 7.3 < O/H < 7.8.
[b] 7.8 < O/H < 8.3.
[c] 8.3 < O/H < 8.8.
[d] Standard reference values (Mg/O = −1.15 dex, Si/O = −1.20 dex, Fe/O = −1.20 dex).
[e] $Mg_{gas}/H = (Si_{gas}/H + Fe_{gas}/H)/2$.
[f] Note that there is an additional 0.03 uncertainty in the absolute calibration, see the text.

So far we have not included the systematic error present in Equation (1) due the depletion determinations of the Orion nebula (our absolute calibrator). This systematic error is comparable to the trends that we have found, and makes any given absolute determination uncertain, but the differences derived between two objects are not affected by this error. The systematic error is about one-fourth of the estimated O depletion and, including the possible errors in the reference values of Mg, Si, and Fe, translates to a final error of 0.03 dex for each of the three intervals discussed in this paper.

8. CONCLUSIONS

From the Mg II 3*d*–4*f* λ4481 recombination line intensities we have derived the Mg/H abundance ratio for the Orion nebula and for 30 Doradus. From this abundance ratio, we have estimated that in the Orion nebula and in 30 Doradus about 9% and 27% of the Mg atoms are in the gas phase, respectively, and that the rest of the Mg atoms are embedded in dust grains.

We have reduced the FORS raw data for SBS 0335−052 E and have measured four of the eight O II lines of multiplet 1 and from the $I(4639 + 4641 + 4649 + 51)/I(H\beta)_{rec} = 0.0231 \pm 0.0111$ value we obtain that $12 + \log(O^{++}/H^{+}) = 7.36^{+0.17}_{-0.28}$ and that the total O/H value amounts to $7.41^{+0.17}_{-0.28}$ dex.

We find that the gaseous Fe/H ratio has a typical value of about 6.25 dex with a dispersion of about 0.30 dex for H II regions with O/H in the 7.3–8.8 dex range. The almost constancy of the gas-phase Fe/H ratio reflects the efficiency of the processes of dust formation and dust destruction. It probably implies that there is a minimum threshold for dust formation given by a gas-phase Fe/H ratio of about 5.8 dex.

Based on the Mg/O, Si/O, and Fe/O abundances of Galactic and extragalactic H II regions we estimate that for the 8.3 dex < O/H < 8.8 dex range the fraction of O atoms trapped by dust grains amounts to 0.11 ± 0.03 dex, for the 7.8 < O/H < 8.3 dex range amounts to 0.10 ± 0.03 dex, and for the 7.3 < O/H < 7.8 dex range amounts to 0.09 ± 0.03 dex. Note that if one of the adopted reference values for Mg, S, and Fe were increased or decreased by 0.1 dex the O depletions mentioned above change by about 0.002 dex.

We also consider that the H II region abundances derived from the *T*(4363/5007) method underestimate the O/H ratio by about 0.15–0.35 dex (e.g., Peimbert & Peimbert 2010b, and

references therein). This result together with the fraction of O atoms embedded in dust grains implies that to obtain the gas-phase plus the dust-phase O/H value it is necessary to increase the O/H gas values derived from the $T(4363/5007)$ method by about 0.25–0.45 dex.

We acknowledge the referee for a careful review of the manuscript and for many excellent suggestions. This work was partly supported by the grants PAPIIT IN123309 from DGAPA (UNAM, Mexico) and CONACyT 46904 (Mexico).

REFERENCES

Asplund, M., Grevesse, N., Sauval, A. J., & Scott, P. 2009, ARA&A, 47, 481
Baldwin, J. A., Ferland, G. J., Martin, P. G., Corbin, M. R., Cota, S. A., Peterson, B. M., & Slettebak, A. 1991, ApJ, 374, 580
Bastin, R. J., & Storey, P. J. 2006, in IAU Symp. 234, Planetary Nebulae in our Galaxy and Beyond, ed. M. J. Barlow & R. H. Méndez (Cambridge: Cambridge Univ. Press), 369
Cannon, J. M., Skillman, E. D., Garnett, D. R., & Dufour, R. J. 2002, ApJ, 565, 931
Carigi, L. 1996, RevMexAA, 32, 179
Carigi, L., & Peimbert, M. 2008, RevMexAA, 44, 341
Carigi, L., & Peimbert, M. 2010, ApJ, submitted, arXiv1004.0756
Chiappini, C., Romano, D., & Matteucci, F. 2003, MNRAS, 339, 63
Deharveng, L., Peña, M., Caplan, J., & Costero, R. 2000, MNRAS, 311, 329
Esteban, C., Bresolin, F., Peimbert, M., García-Rojas, J., Peimbert, A., & Mesa-Delgado, A. 2009, ApJ, 700, 654
Esteban, C., García-Rojas, J., Peimbert, M., Peimbert, A., Ruiz, M. T., Rodríguez, M., & Carigi, L. 2005, ApJ, 618, L95
Esteban, C., Peimbert, M., García-Rojas, J., Ruiz, M. T., Peimbert, A., & Rodríguez, M. 2004, MNRAS, 355, 229
Esteban, C., Peimbert, M., Torres-Peimbert, S., & Escalante, V. 1998, MNRAS, 295, 401
Esteban, C., Peimbert, M., Torres-Peimbert, S., & Rodríguez, M. 2002, ApJ, 581, 241
Fadeyev, Y. 1988, in Atmospheric Diagnostics of Stellar Evolution, ed. K. Nomoto (Berlin: Springer), 533
García-Rojas, J., Esteban, C., Peimbert, A., Peimbert, M., Rodríguez, M., & Ruiz, M. T. 2005, MNRAS, 362, 301
García-Rojas, J., Esteban, C., Peimbert, A., Rodríguez, M., Peimbert, M., & Ruiz, M. T. 2007, RevMexAA, 43, 3
García-Rojas, J., Esteban, C., Peimbert, M., Costado, M. T., Rodríguez, M., Peimbert, A., & Ruiz, M. T. 2006, MNRAS, 368, 253
García-Rojas, J., Esteban, C., Peimbert, M., Rodríguez, M., Ruiz, M. T., & Peimbert, A. 2004, ApJS, 153, 501
Garnett, D. R., Dufour, R. J., Peimbert, M., Torres-Peimbert, S., Shields, G. A., Skillman, E. D., Terlevich, E., & Terlevich, R. J. 1995, ApJ, 449, L77
Izotov, Y. I., Chaffee, F. H., Foltz, C. B., Green, R. F., Guseva, N. G., & Thuan, T. X. 1999, ApJ, 527, 757
Izotov, Y. I., Guseva, N. G., Fricke, K. J., & Papaderos, P. 2009, A&A, 503, 61
Izotov, Y. I., Stasińska, G., Meynet, G., Guseva, N. G., & Thuan, T. X. 2006, A&A, 448, 955
Izotov, Y. I., & Thuan, T. X. 1998, ApJ, 500, 188
Izotov, Y. I., & Thuan, T. X. 2004, ApJ, 602, 200
Izotov, Y. I., Thuan, T. X., & Lipovetsky, V. A. 1997, ApJS, 108, 1
Jenkins, E. B. 2009, ApJ, 700, 1299
Keenan, F. P., Aller, L. H., Ryans, R. S. I., & Hyung, S. 2001, Proc. Natl Acad. Sci. USA, 98, 9476
Liu, Y., Liu, X.-W., Barlow, M. J., & Luo, S.-G. 2004, MNRAS, 353, 1251
López-Sánchez, A. R., Esteban, C., García-Rojas, J., Peimbert, M., & Rodríguez, M. 2007, ApJ, 656, 168
Luridiana, V., Peimbert, A., Peimbert, M., & Cerviño, M. 2003, ApJ, 592, 846
Mesa-Delgado, A., Esteban, C., García-Rojas, J., Luridiana, V., Bautista, M., Rodríguez, M., López-Martín, L., & Peimbert, M. 2009, MNRAS, 395, 855
Nuth, J. A., & Hecht, J. H. 1990, Ap&SS, 163, 79
Ossenkopf, V., Henning, Th., & Mathis, J. S. 1992, A&A, 261, 567
Pagel, B. E. J. 2009, Nucleosynthesis and Chemical Evolution of Galaxies (2nd ed.; Cambridge: Cambridge Univ. Press)
Pagel, B. E. J., & Tautvaisiene, G. 1995, MNRAS, 276, 505
Peimbert, A. 2003, ApJ, 584, 735
Peimbert, A., & Peimbert, M. 2005, RevMexAASC, 23, 9
Peimbert, A., & Peimbert, M. 2010a, in IAU Symp. 268, Light Elements in the Universe, ed. C. Charbonnel et al. (Cambridge: Cambridge Univ. Press), 185
Peimbert, A., Peimbert, M., & Ruiz, M. T. 2005, ApJ, 634, 1056
Peimbert, M. 1967, ApJ, 150, 825
Peimbert, M., & Costero, R. 1969, Bol. Obs. Tonantzintla Tacubaya, 5, 3
Peimbert, M., Luridiana, V., & Peimbert, A. 2007, ApJ, 666, 636
Peimbert, M., & Peimbert, A. 2010b, RevMexAASC, in press, arXiv:0912.3781
Peimbert, M., Peimbert, A., & Ruiz, M. T. 2000, ApJ, 541, 688
Perinotto, M., & Patriarchi, P. 1980, ApJ, 235, L13
Pilyugin, L. S., Ferrini, F., & Shkvarun, R. V. 2003, A&A, 401, 557
Przybilla, N., Nieva, M. F., & Butler, K. 2008, ApJ, 688, L103
Rodríguez, M., & Rubin, R. H. 2005, ApJ, 626, 900
Ruiz, M. T., Peimbert, A., Peimbert, M., & Esteban, C. 2003, ApJ, 595, 247
Simón-Díaz, S. 2010, A&A, 510, 22
Storey, P. J. 1994, A&A, 282, 999
Storey, P. J., & Hummer, D. G. 1995, MNRAS, 272, 41
Thuan, T. X., Izotov, Y. I., & Lipovetsky, V. A. 1997, ApJ, 477, 661
Tsamis, Y. G., & Péquignot, D. 2005, MNRAS, 364, 687